BIOCHEMISTRY
including biophysical chemistry & molecular biology

Article

pubs.acs.org/biochemistry

Exploring the Role of Conformational Heterogeneity in *cis*-Autoproteolytic Activation of ThnT

Andrew R. Buller,[†,∥] Michael F. Freeman,[‡,⊥] Joel F. Schildbach,[§] and Craig A. Townsend*[,†,‡,§]

[†]Department of Biophysics, Johns Hopkins University, Baltimore, Maryland 21218, United States
[‡]Department of Chemistry, Johns Hopkins University, Baltimore, Maryland 21218, United States
[§]Department of Biology, Johns Hopkins University, Baltimore, Maryland 21218, United States

Supporting Information

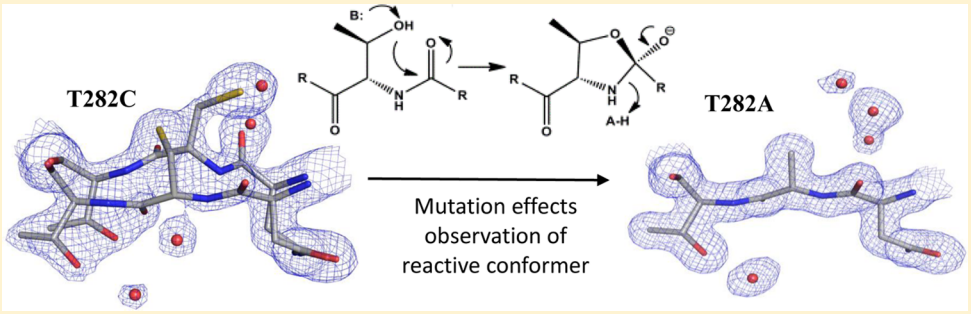

ABSTRACT: In the past decade, there have been major achievements in understanding the relationship between enzyme catalysis and protein structural plasticity. In autoprocessing systems, however, there is a sparsity of direct evidence of the role of conformational dynamics, which are complicated by their intrinsic chemical reactivity. ThnT is an autoproteolytically activated enzyme involved in the biosynthesis of the β-lactam antibiotic thienamycin. Conservative mutation of ThnT results in multiple conformational states that can be observed via X-ray crystallography, establishing ThnT as a representative and revealing system for studing how conformational dynamics control autoactivation at a molecular level. Removal of the nucleophile by mutation to Ala disrupts the population of a reactive state and causes widespread structural changes from a conformation that promotes autoproteolysis to one associated with substrate catalysis. Finer probing of the active site polysterism was achieved by EtHg derivatization of the nucleophile, which indicates the active site and a neighboring loop have coupled dynamics. Disruption of these interactions by mutagenesis precludes the ability to observe a reactive state through X-ray crystallography, and application of this insight to other autoproteolytically activated enzymes offers an explanation for the widespread crystallization of inactive states. We suggest that the N → O(S) acyl shift in *cis*-autoproteolysis might occur through a *si*-face attack, thereby unifying the fundamental chemistry of these enzymes through a common mechanism.

Understanding the interplay between conformational dynamics and the population of reactive states is a central challenge in biocatalysis. This pursuit has yielded major successes in the past 15 years via the combination of diverse techniques such as X-ray crystallography to define static protein states with enzyme kinetics or solution spectroscopy to probe catalytically relevant dynamic motions.[1−5] Studies of model systems have demonstrated the importance of motions on a huge range of time scales, from femtoseconds[6,7] to milliseconds.[8,9] These strategies have been supported by the use of substrate analogues and transition state mimics that allow direct interrogation of high-energy states.[10,11] Many of these techniques, however, are not suited to the study of large autoprocessing systems, which possess intrinsic, unimolecular chemical reactivity upon formation of a folded state. Autoprocessing is implicated in diverse physiological processes such as signal transduction,[12,13] nucleoporin biogenesis,[14,15] RNA self-splicing,[16] protein folding,[17,18] and formation of enzyme catalysts.[19,20] Because of their intramolecular nature, autoprocessing reactions constitute one of the most simple structure−function relationships in biochemistry. Despite this fact there have been few links established between their inherent structural plasticity and the chemical reactions they evolved to accelerate.

Autoproteolysis is a common post-translational modification that proceeds through an N → O(S) acyl shift mechanism (Figure 1). A nucleophilic residue attacks into its N-terminal peptide bond, forming a five-membered (thia)oxazolidine ring, which collapses to a (thio)ester. This acyl migration is identical to the first step of intein splicing[21] but differs in autoproteolysis in that the (thio)ester intermediate is hydrolyzed to produce an N-terminal nucleophile (Ntn). The nascent α-amine generated by this chemistry is the base in a noncanonical catalytic diad whose reactivity is tuned by neighboring interactions.[19,22] A key

Received: March 29, 2014
Revised: June 3, 2014
Published: June 16, 2014

   dx.doi.org/10.1021/bi500385d | *Biochemistry* 2014, 53, 4273−4281

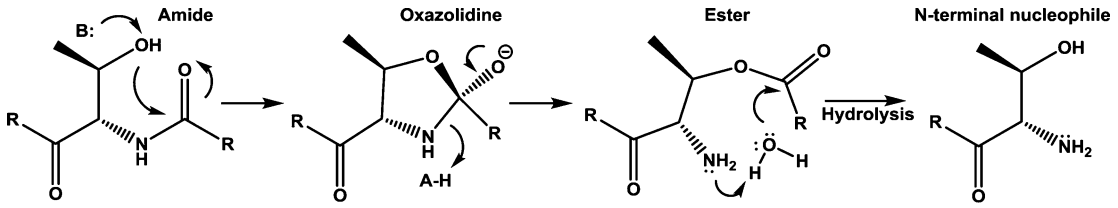

Figure 1. Autoproteolysis mechanism with a Thr nucleophile. Activation of the nucleophile allows attack into its N-terminal amide bond, forming a five-membered ring. Protonation of the amine leaving group facilitates collapse to form an ester intermediate, which is subsequently hydrolyzed. Dissociation of the new C-terminus yields an N-terminal nucleophile used in substrate catalysis.

development in our understanding of autoproteolytic enzymes was the discovery that penicillin acylase,[23] glutamine PRPP amidotransferase,[24] and the proteasome β-subunit (PβS)[25] have a common Ntn fold and a shared evolutionary history.[19] This group of enzymes is now designated clan PB according to the MEROPS nomenclature.[26] Early clues about autoproteolysis came from the study of PβS. The structure of a fully assembled 20S proteasome with a Thr → Ala mutation showed the system was poised for *si*-face attack.[27] However, all subsequent research into the autoproteolysis of clan PB has implicated activation through a *re*-face attack, a proposal that precludes utilization of the enzymatic oxyanion hole. These conclusions imply that proteins with a shared lineage use two fundamentally different mechanisms for the same chemistry. While possible, our recent discovery that the stereochemistry of catalysis for Ser, Cys, and Thr proteases is absolutely conserved throughout divergent evolution demands that special consideration be given to the evidence supporting divergence of mechanism.[28]

While studying the biosynthesis of the β-lactam antibiotic thienamycin, we reported that the *cis*-autoproteolytic enzyme ThnT acts late in the biosynthetic pathway as a pantetheine hydrolase.[29] ThnT is a member of clan PE and is therefore related to hydrolases from clan PB through convergent evolution. By mutating the active site nucleophile of ThnT from Thr to Cys, we prepared a chemically stable variant that was capable of undergoing a very slow N → S acyl shift.[30] The X-ray structure of ThnT T282C was a dimer with two conformations at the active site of the π_1 subunit (Figure 2A), and a single conformation in the π_2 subunit. The observation of multiple states at the active site raised the important question of which conformation, if either, corresponds to a reactive state. Comparison to the convergently related Ntn hydrolases revealed the major conformer in the ThnT T282C structure was almost identical to the precleavage structures of the penicillin and cephalosporin acylases, which were proposed to autoproteolyze through a *re*-face attack. However, the minor conformer in the ThnT T282C active site was similar to the uncleaved PβS enzyme, the only Ntn enzyme proposed to mature through a *si*-face attack. We applied simple mechanistic criteria to determine which of these states might give rise to chemistry: the ability of the wild-type nucleophile to populate a reactive rotamer, a well-formed oxyanion hole, and the presence of proton donors or acceptors for the nucleophilic hydroxyl and amide nitrogen leaving group. This analysis strongly supported the assignment of the minor conformer of ThnT T282C as the reactive state for *cis*-autoproteolysis. Moreover, we found circumstantial evidence that the penicillin and cephalosporin acylases undergo a hidden conformational rearrangement to prime their active sites for *si*-face attack. These data demonstrated the relevance of protein dynamics in establishing a chemically sound mechanism for autoprocessing. Additionally, analysis of γ-glutamyltranspeptidase,[31] L-asparaginase,[32] and Taspase1[33] showed they crystallized in inactive states, but there was not enough information to suggest the nature of their reactive conformation, raising the question of why X-ray crystallography so rarely captures reactive states in autoproteolytic systems.

We suspected that most self-cleavage chemistry is initiated from a high-energy conformation and that some rearrangement must occur to populate this state. The serendipitous observation of both active and inactive states of ThnT provides a unique opportunity to study the links between structural dynamics and autoprocessing chemistry. We used a structural and kinetic approach to establish that large conformational fluctuations in three regions of ThnT are coupled to one another and that multiple states of this ensemble contribute to the observed autoproteolysis rate. Our data establish that mutation may slow autoproteolysis both by reducing the rate of transition state stabilization and by biasing the ensemble toward less reactive states. Therefore, the conditions used to impede autoprocessing for structural characterization can reduce the population of the high-energy reactive states such that they are impossible to observe through X-ray crystallography, thereby explaining the overwhelming tendency of autoprocessing systems to crystallize in inactive forms.

EXPERIMENTAL PROCEDURES

Expression Vector Construction. Codon-optimized ThnT was expressed from a plasmid described previously.[29] Overlap extension polymerase chain reaction was used to create the S320A and N281A mutations using primer sequences listed in Table S1 of the Supporting Information. Because of internal complementarity within the ThnT gene, conventional primers for mutation of Pro78 resulted in a large internal deletion. This aberrant amplification was circumvented by designing primers that contained a codon-optimized synthon harboring the desired mutation. Products were gel purified, digested with NdeI and HindIII restriction enzymes (New England Biolabs), and ligated into pET28b(+) (EMD Biosciences), yielding N-6His tag fusions. All mutant genes were sequence-verified and transformed into *Escherichia coli* Rosetta2(DE3) electrocompetent cells (EMD Biosciences).

Protein Expression and Purification. Expression and purification of all ThnT proteins were similar to reported procedures.[34] Proteins were bound to a Ni-nitriloacetate column and eluted in 250 mM imidazole, 50 mM sodium phosphate (pH 7.5), 40 mM NaCl, and 10% glycerol. Protein was concentrated in a 10 KDa molecular weight cutoff Amicon filtration device (Bio-Rad) and buffer exchanged into 10 mM potassium phosphate (pH 7.5) with 10% glycerol (for kinetic experiments) or 20 mM potassium phosphate (pH 7.5) with 5% glycerol (for crystallography). Protein was passed through 1 mL Q-Sepharose anion exchange resin and reconcentrated

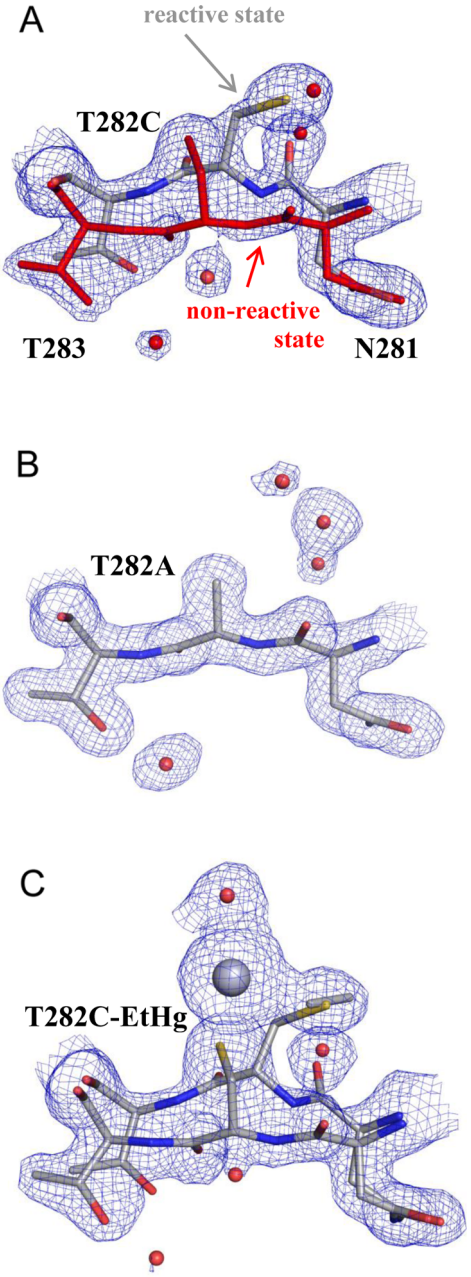

Figure 2. Electron density at the active site of the π_1 subunit of mutationally inactivated ThnT variants. (A) Two conformations corresponding to reactive and inactive states observed in the structure of T282C. (B) Only the inactive, state B, is found in the structure of T282A. (C) Derivatization of C282 with EtHg causes a shift in the electron density of the active site toward state B. Occupancy refinement indicates reactive state A is still populated at ~30% occupancy. The $2mF_o - DF_c$ maps are contoured at 1.0σ.

before being stored at −80 °C. Purification at 4 °C was critical for wild-type ThnT to capture enough of the precursor protein for quantification.

Autoproteolysis Kinetics and Eyring Analysis. Purified ThnT was diluted to a concentration of 1 μg/μL in 100 mM Tris (pH 7.5), 100 mM KCl, and 10% glycerol and preheated in a water bath for 2 min before a time course was begun. We initially observed that long incubations of ThnT variants in phosphate buffer resulted in degradation that would preclude the long time courses necessary to measure slow reaction rates. The inclusion of a protease inhibitor cocktail halted some degradation, and switching to a Tris buffer further increased the stability of the system, allowing quantification of slow reaction rates (Figure S1 of the Supporting Information). For each time point, protein was denatured in sodium dodecyl sulfate loading buffer and heated to 98 °C for 2 min. Samples were subjected to 15% sodium dodecyl sulfate−polyacrylamide gel electrophoresis and quantified with ImageJ. Autoproteolysis kinetics for each ThnT variant were run in triplicate at 37 °C and quantified with Prism and fit to eq 1.

$$y = (A - C)e^{-kT} + C \quad (1)$$

Given that the pK_a of Tris is temperature sensitive, special care was taken to adjust the pH of each buffer at the desired temperature for Eyring analysis. Each measurement was performed at least twice, and the data were fit to the Eyring−Polanyi equation (eq 2) in Prism.

$$\ln\left(\frac{k}{T}\right) = -\frac{\Delta H^{\ddagger}}{R} \times \frac{1}{T} + \ln\left(\frac{k_B}{h}\right) + \frac{\Delta S^{\ddagger}}{R} \quad (2)$$

Crystallization and Data Collection. Trays for sitting-drop vapor diffusion were prepared with ThnT T282A concentrated to 7.7 μg/μL, against a 1 mL reservoir of 17−25% PEG3350 and 0.15−0.4 M sodium acetate. Crystals were cryoprotected by immersion in 22% PEG3350, 0.3 M sodium acetate, and 20% glycerol and immediately flash-frozen in liquid N_2. Diffraction data were collected on NSLS X6A at the Brookhaven National Laboratory (Upton, NY). To reduce reflection overlap, 1050 frames with a 0.2° oscillation were collected, yielding 210° of data that were processed in HKL2000.[35]

Diffraction data for the T282C EtHg-derivatized structure were described previously.[30] We hypothesized that longer soaks of T282C crystals in 200 μM ethylmercuric phosphate would result in greater incorporation of the EtHg and thereby further shift the conformational ensemble within the structure. Unfortunately, soaking crystals for longer periods of time resulted in derivatization at additional sites.

Structure Solution, Model Building, and Refinement. Direct multiple-wavelength anomalous diffraction phase information was used for the solution of the T282C EtHg-derivatized structure. The structure of T282A was determined by molecular replacement using Phaser,[36] using the T282C variant of ThnT [Protein Data Bank (PDB) entry 3S3U] with all active site and dual occupancy residues removed from the search model. Iterative model building in Coot[37] and refinement in Refmac5[38] yielded readily interpretable maps. As higher-resolution data were incorporated, it became clear that systematic absences from the model corresponded to conformations described in previously determined structures. These states were modeled in Coot, and their occupancy was systematically varied by increments of 5% before restrained refinement in Refmac5. The low-occupancy conformation whose *B* factors were approximately equal to the major conformer was included in the model only if its geometry also refined within canonical values. TLS operators were included in the final round of refinement, as implemented in Refmac5.[39] Crystallographic and model statistics are listed in Table S2 of the Supporting Information.

dx.doi.org/10.1021/bi500385d | *Biochemistry* 2014, 53, 4273−4281

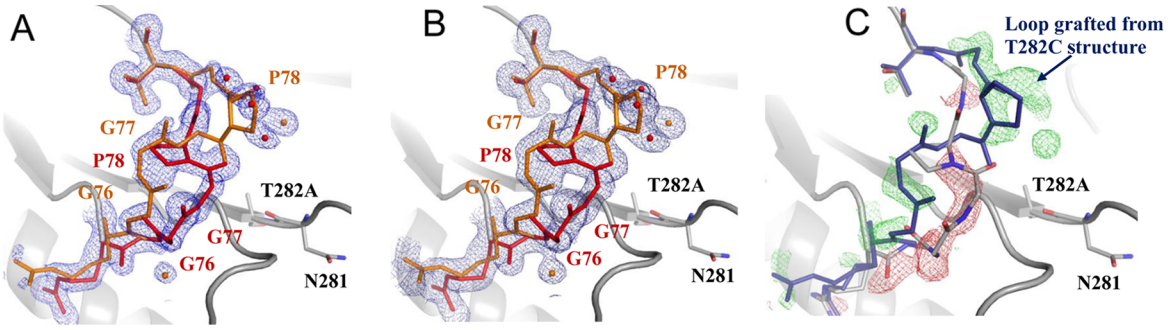

Figure 3. Multiple conformations in residues R74–T80 are adjacent to the active site of T282A. The $2mF_o - DF_c$ map at (A) 1.0σ and (B) 0.5σ shows the predominant state (red) with the *trans* isomer of the G77–P78 peptide bond. The low-occupancy conformation (orange) features the *cis* isomer of the G77–P78 peptide bond. (C) $F_o - F_c$ map contoured at 3.0σ from a model built of T282A at 1.5 Å resolution with only the major conformer. Negative density (red) indicates this conformation is not fully occupied, and systematic peaks in the positive density (green) clearly correspond to the conformer captured in the T282C structure (blue sticks).

RESULTS

Systematic Structural Changes Are Caused by Removal of the Nucleophile. We hypothesized that the reactive state identified in the T282C structure of ThnT was stabilized by the hydrogen bonding characteristics of the thiol, which mimic those of the naturally occurring hydroxyl group. To test this proposal, we expressed and purified ThnT T282A, which does not undergo autoproteolysis and was amenable to crystallization. Crystals of T282A grew in conditions comparable to those used for the T282C variant and diffracted well, and molecular replacement readily yielded a high-resolution structure. Consistent with our hypothesis, the 1.5 Å crystal structure of T282A showed no electron density corresponding to the reactive state in either subunit of the protein (Figure 2B). Instead, the oxyanion hole was filled by a network of water molecules. van der Waals constraints imply these water molecules were too close to be present simultaneously, indicating that multiple modes of water occupation are possible within the cavity created by the T282A mutation.

During model building and refinement, it became clear that a glycine-rich loop adjacent to the active site, composed of residues R74–T80 (RGGGPGT), adopted a conformation dramatically different from that observed in the T282C structure (Figure 3A,B). This unanticipated conformation was identical to that observed in the postautoproteolysis structure of wild-type ThnT and is necessary for substrate binding in the mature enzyme.[34] Stepwise inclusion of higher-resolution data during model refinement resulted in numerous peaks in the $F_o - F_c$ map indicative of structural heterogeneity (Figure 3C). Given that modeling of weak density results in a phase bias, we were concerned that modeling with multiple conformations would be impossible. However, we found that all of the positive omit peaks systematically matched the conformation originally described in the structure of T282C (Figure 3C). Therefore, grafting this well-defined model into the T282A structure did not rely on weak density for the initial build. Refinement of this alternative state generated poor geometry when the resolution was above 1.75 Å but resulted in excellent geometry and packing with the full 1.5 Å data set, as measured by MolProbity.[40] Refinement with the occupancy of the minor conformer set at 30% yielded average *B* factors that were approximately equal in each state (Figure 3B; 14.9 Å^2 for the major state and 14.5 Å^2 for the minor state).

Multiple States within the Conformational Ensemble Contribute to Autoproteolysis. These two conformations differ at the G77–P78 peptide bond, which undergoes transitions between the *cis* and *trans* isomers. The *trans* isomer dominates in the structure of T282A and is the only one observed in the postautoproteolysis wild-type enzyme.[34] The *cis* isomer is more prevalent in the T282C structure, and we hypothesized that it facilitates efficient autoprocessing. Specifically, the data show that the backbone carbonyl of Gly77 in the *cis* isomer positions a water molecule to aid in the activation of the nucleophile for the N → O acyl shift.[30] The different physical properties of the *cis* and *trans* isomers of the peptide bond provide a convenient means of experimentally testing the role of the R74–T80 loop dynamics in autoproteolysis. If the *cis* conformation were strictly necessary for autoproteolysis, then the P78G and P78A mutations would intrinsically favor the *trans* isomer by >300-fold[41] and slow autoproteolysis by a corresponding amount. We constructed these variants and observed a relatively small, 10-fold rate deceleration for the P78G mutant relative to that of the wild type (Table 1). This effect is even smaller for P78A and is consistent with our hypothesis that the *cis* conformation of the R74–T80 loop accelerates autoproteolysis but indicates that it is not strictly necessary. Surprisingly, the ΔP78 deletion variant autoproteolyzed faster than either of the point mutants but was still slower than the wild type. Because this loop occurs at the surface of the protein, these data suggest that the role of G76 in activating the nucleophile is rescued by interactions with the solvent when the *cis* conformation is not populated.

Table 1. Kinetic Parameters for ThnT Autoproteolysis[a]

protein	k_{obs} (min^{-1})	$\Delta\Delta G^{\ddagger}$ (kcal/mol)
wild-type	0.0140 ± 0.0016	
P78G	0.00134 ± 0.00013	1.45 ± 0.13
P78A	0.00323 ± 0.00005	0.91 ± 0.08
ΔP78	0.0059 ± 0.0004	0.54 ± 0.11
N281A	0.0017 ± 0.0004	1.33 ± 0.18
S320A	0.0045 ± 0.0007	0.62 ± 0.16
N281A/S320A	0.00087 ± 0.0006	1.72 ± 0.11

[a]Autoproteolysis rates of ThnT variants at 37 °C. Rate values are a weighted average of at least three independent measurements with their standard deviation given.

Additionally, the collapse of the R74–T80 loop into the *trans* conformation appeared to influence the structure of a short

dx.doi.org/10.1021/bi500385d | *Biochemistry* 2014, 53, 4273–4281

loop composed of residues L318−D321 (Figure S2 of the Supporting Information). This motif was observed in two conformations in the T282C structure but instead populates a single conformation in the T282A structure that most closely resembled the structure of ThnT after autoproteolysis occurs. This rearrangement may be rationalized by recognizing that G76 in the *trans*-configured state would form a steric clash with L319 if some rearrangement did not occur. Further insight into these interactions was hampered by both the complexity of the large transitions observed upon mutational removal of the nucleophile and the introduction of a non-native water network into the cavity caused by this mutation. Therefore, we sought a more subtle means of probing how population of the reactive state influences the protein ensemble.

Probing Dynamics through Mutagenesis and Chemical Derivatization of the Nucleophile. One powerful means of identifying structural changes relevant to catalysis is to titrate a substrate analogue or transition state mimic and monitor changes in the structure and dynamics. This approach is not possible for autoprocessing reactions, which are limited by the chemical moieties present on the proteinogenic amino acids. Instead, we attempted to exploit the unique reactivity of the thiol present in the active site of the T282C variant of ThnT. We hypothesized that chemical derivatization of the nucleophile would trap the protein in its inactive state without creating the cavity caused by the T282A mutation. Previous phasing experiments of ThnT relied on a heavy atom soak of T282C with ethylmercury phosphate. Model building from these data at 1.65 Å resolution indicated ∼45% incorporation of the EtHg, with the Hg atom covalently linked to the thiol of T282C. This derivatized species was clearly trapped in the inactive state (Figure 2C).

Difference density corresponding to the active state was still observable, and a refinement procedure identical to that used to model the R74−T80 loop was used to assign an occupancy of 30%. Multiple conformations of the L318−D321 loop were still detected; however, the electron density showed a clear shift in the relative population of these states (Figure 4A,B). This trend continues when including the π_2 subunit of ThnT, where only the inactive state is observed and a single conformation of the L318−D321 loop is present with a water-mediated hydrogen bond between S320 and N281 (Figure 4C). We identified two factors that may contribute to the molecular basis for this interaction. When the L318−D321 loop is away from the active site, the "Out" conformation, there is a water-mediated hydrogen bond between N281 and S320. This bound water molecule is expelled when the L318−D321 loop moves ∼1.5 Å closer to the active site and a direct hydrogen bond is formed between S320 and N281. This "In" conformation has a 2.5 Å steric clash between the carbonyl of S320 and the scissile bond in its inactive state B (Figure 4A). These crystallographic data suggest a model in which the favorable expulsion of water at the S320−N281 interface destabilizes the inactive state B and promotes rearrangement of the active site into a high-energy state primed for autoproteolysis.

The hydrogen bonding interactions in the S320−N281 interface do not appear to directly participate in the chemistry of autoproteolysis (Figure 4). Nonetheless, measurement of the autoproteolysis rates for the Ala variant at each position showed they both slowed self-cleavage, with N281A autoproteolysis 2.6-fold slower than S320A (Table 1). The N281A mutation opens a large space close to the site of amine protonation, and altered solvation may affect amine reactivity during the N → O acyl

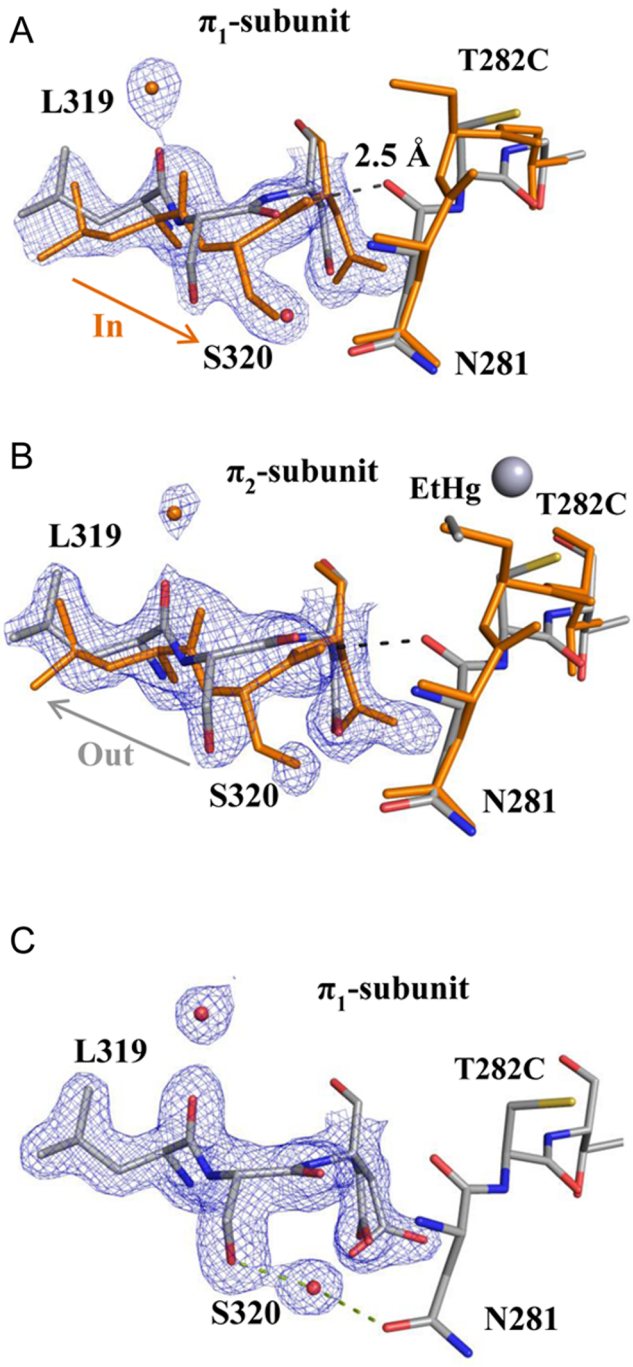

Figure 4. Population shifts in the L319−D321 region are associated with the state of the active site. (A) Two conformations originally discovered in the structure of T282C, with the "In" state favored. (B) Derivatization of the nucleophile traps the inactive state B, which in turn causes a shift in the population of the L319−D321 region toward an "Out" state. (C) When state B is exclusively populated, only the "Out" state is observed.

shift. However, the S320A variant maintains the chemical environment of the active site. Its decelerated autoproteolysis is consistent with the hypothesis that conformational coupling between N281 and S320 stabilizes the reactive state. We attempted to measure the nonadditivity in the effect of an N281A/S320A double variant, which would provide an estimation of the coupling energy contributing to autoactivation. However, the rate differences were too small relative to

dx.doi.org/10.1021/bi500385d | *Biochemistry* 2014, 53, 4273−4281

the error of the measurements to make a statistically significant statement.

Determination of the Activation Parameters of Autoproteolysis. The polysterism we observed in these mutationally inactivated structures of ThnT involves large backbone-level fluctuations. Although we do not know the frequency at which these transitions occur, it is typical that such motions take place on the millisecond time scale.[42,43] Given that these motions are fast relative to autoproteolysis ($t_{1/2}$ = 50 min), we posit that the states we observed through X-ray crystallography are in a pseudothermodynamic equilibrium prior to autoprocessing. If these states are populated at a significant level prior to autoproteolysis, then selection for the reactive state will be entropically unfavorable. To test whether this phenomenon is possible, we subjected the wild-type ThnT to Eyring analysis to determine the activation parameters of autoproteolysis.

We measured the ThnT autoproteolysis rate between 52 and 27 °C and fit the data to the Eyring–Polyani equation (Figure 5). The $\Delta H^{\ddagger}$ of ThnT was 18.1 ± 0.5 kcal/mol, and the $T\Delta S^{\ddagger}$

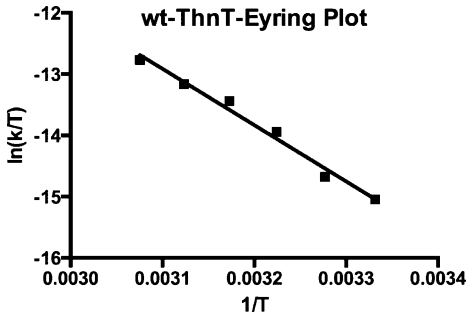

Figure 5. Eyring plot of ThnT autoproteolysis. Each point represents a weighted average of at least two independent measurements. See Experimental Procedures for details.

was −5.0 ± 0.5 kcal/mol at 37 °C, indicating that entropy effects play a significant role in the autoactivation of ThnT. Whether this unfavorable change in entropy reflects decreasing degrees of solvent or protein freedom is difficult to determine, and sophisticated NMR techniques for measuring protein conformational entropy are just now emerging.[44]

DISCUSSION

Mechanistic Importance of Conformational Dynamics in ThnT Autoactivation. Our initial study of ThnT autoproteolysis revealed a reactive state formed through active site conformational rearrangement and found that the majority of pro-enzyme structures do not represent a reactive state.[30] This investigation was driven by two related questions: How do conformational dynamics relate to ThnT function, and why do other pre-autoprocessing structures rarely display reactive conformations? We hypothesized that the conserved hydrogen bond capabilities of T282C stabilize the reactive state of ThnT, and our first experiment was to observe what happens when this group was removed.

The structure of T282A at 1.5 Å resolution showed a complete lack of electron density corresponding to the reactive state (Figure 2B). Given that this conformation was present at 55% occupancy in the 1.6 Å structure of T282C (Figure 2A), destabilization by as few as 0.5 kcal/mol would be sufficient to render this state invisible to X-ray crystallography. Recent investigations have demonstrated that "noise" in the electron density is statistically enriched in biologically relevant side chain conformations,[1,45,46] and we expand upon these studies with the structure of T282A, which contains a low-occupancy conformer of that R74–T80 loop indicative of a large backbone-level rearrangement. Kinetic experiments support the idea that this alternative conformation contributes to the observed autoproteolysis rate, affirming the biological relevance of low-occupancy states that can be observed in high-resolution X-ray structures.

The second site of conformational coupling that we observed was the interface between N281 and S320. The structure of T282C showed multiple conformations in the L318–D321 loop, suggesting it might be sensitive to the population of the reactive state. In most crystallographic studies, a causal relationship cannot be established between the population of multiple conformational states. Two factors allowed us to overcome this limitation. First, there is a steric clash between the backbone of S320 and the scissile bond in its nonreactive conformation, establishing that these states cannot be populated at the same time. Second, site-specific derivatization with EtHg trapped the active site in its inactive state, while all other features of the structures remained constant. Therefore, the observed shift in the population of the L318–D321 loop was caused by the derivatization.

We hypothesize that population of the "In" state of the L318–D321 loop is stabilized by the release of water and a hydrogen bond between the S320 and N281 side chains but causes a steric clash with the carbonyl of the scissile bond. This clash promotes the peptide flip necessary to place the reactive amide into the oxyanion hole. Mutational disruption of the S320–N281 interface slows autoproteolysis and supports our model of how protein conformational dynamics influence population of the reactive state.

Exploring Entropy Changes during Autoactivation. Each of the conformational states captured in our X-ray structures differs at the level of the backbone, and motion between them is likely near the millisecond time scale.[42,43] Therefore, each of these states possesses a unique manifold of rotameric substates that may interconvert on a relatively fast time scale. This scenario allows an interesting possibility, that selection for the reaction state causes a change in the protein conformational entropy. Conformational entropy has been dubbed the "dark energy" of proteins,[47] and its role in governing ligand binding has only recently been experimentally verified.[44] It would be of significant fundamental interest to extend this advance into protein chemistry, and we performed Eyring analysis of ThnT to collect as many relevant data as possible on this phenomenon.

We found that the $T\Delta S^{\ddagger}$ at 37 °C contributes 5.0 kcal/mol to the activation barrier of ThnT autoproteolysis. Because the chemistry in question is unimolecular, this restriction on the degrees of freedom in the transition state can come from only protein or solvent, significantly simplifying the analysis. Unfortunately, the activation parameters of uncatalyzed *cis*-autoproteolysis through the acyl shift reaction are not known because direct hydrolysis is favored in solution.[48] The activation parameters for glycosylasparaginase (GA) from *Flavobacterium meningosepticum* showed the barrier to autoproteolysis is entirely enthalpic ($\Delta H^{\ddagger}$ = 22 kcal/mol, and $T\Delta S^{\ddagger} \sim 0$ kcal/mol at 37 °C).[49] Because GA shares the same uncatalyzed rate of autoproteolysis with ThnT, the difference in their activation parameters must reflect protein-specific entropic contributions to rate enhancement. Further insights into conformational

entropy are not readily accessible through crystallography or mutagenesis, and we look forward to the application of additional techniques to study this problem.

Effects of Mutagenesis on the Observation of Reactive States. The Boltzmann distribution allows for all states to be populated at some level, but only those within ≈0.7 kcal/mol of the global minimum can be seen with a high-resolution crystal structure. Given that autoprocessing chemistry proceeds from high-energy states, our kinetic data establish that the $\Delta\Delta G^{\ddagger}$ values of the least disruptive mutations are sufficient to shift the ensemble so that the reactive state is no longer observable. Even without mutational disruption, the reactive state of an autoprocessing system may be insufficiently populated for characterization by X-ray crystallography. Indeed, this exact scenario hindered study of the hammerhead ribozyme, a self-cleaving RNA molecule. A construct that could react in the crystal gave rise to a structure that corresponded to a nonreactive conformation.[50,51] Investigators recognized mechanistic inconsistencies implied by the structural data, and a decade of research finally yielded a structure corresponding to a reactive state.[16,52,53] Given this cautionary lesson in the interpretation of "reactive" crystal structures, we searched for chemical constraints that have not been satisfied in the mechanisms suggested by inactivated pro-enzyme structures, which might indicate nonreactive protein conformations.

Critical Re-evaluation of Reactive States in Autoproteolytic Enzymes. The autoactivation of only one enzyme other than ThnT from clan PE has been studied. The Nuc → Ala variant of β-aminopeptidase (BapA) crystallized in a conformation comparable to the inactive state of ThnT.[54] From these data, it was proposed that BapA did not undergo the canonical N → O acyl shift mechanism, but rather an unprecedented *trans*-type autoproteolysis. This proposal, while provocative, lacked the discriminating experiment in which the Nuc → Cys variant is chemically rescued by addition of hydroxylamine.[55] Moreover, the active site architecture for the proposed Ser288 acylation is entirely unprecedented compared to that of canonical Ser proteases,[28] and the mechanism fails to account for protonation of the amine leaving group. Until firm biochemical data exist to overturn the deeply precedented N → O acyl shift mechanism (Figure 1), it should be assumed that autoactivation of all members from clan PE will proceed through *cis*-autoproteolysis with a *si*-face attack on the scissile bond, as has been described for ThnT. This proposal is consistent with the observation that the stereochemistry of catalysis in Ser, Cys, and Thr proteases is conserved throughout divergent evolution.[28]

Extensive study of enzymes from clan PB has yielded two fundamentally different mechanisms for their *cis*-autoproteolysis. The proteasome β-subunit (PβS) autoprocessing is initiated through a *si*-face attack that utilizes the enzymatic oxyanion hole.[27] Although the original interpretations of the penicillin and cephalosporin acylase enzymes from clan PB supported a *re*-face attack mechanism, our previous analysis showed this was unlikely to be the case and found strong circumstantial evidence supporting *si*-face attack.[30]

Alternatively, glycosylasparaginase (GA) is proposed to self-activate through a *re*-face attack generating an oxyanion that is not stabilized by the enzymatic oxyanion hole.[56] This mechanism for GA is supported by the structure of a Thr → Cys variant of the nucleophile that is reactive within the crystal. Given that such reactivity is not a sufficient criterion for the structural assignment of a reactive state, it remains that GA could undergo an as-yet-uncharacterized rearrangement that places the scissile bond in the catalytic oxyanion hole, thus priming the system for *si*-face attack. More recent studies of the human L-asparaginase (ASNase) enzyme have also implicated a *re*-face attack.[57] This proposal was generated through inspection of the structure of the wild-type enzyme, which undergoes self-activation so slowly that it can be crystallized prior to autoproteolysis. Independent analysis of these structures shows the nucleophile is separated from the scissile bond by >4.0 Å and that the extended geometry of the active site is ill-suited for oxazolidine formation. From these mechanistic constraints, we conclude these structures of human ASNase cannot represent a mechanistically relevant state and that some structural rearrangement must occur prior to autoproteolysis. This analysis is supported by the structure of a type III guinea pig ASNase (which is 79.9% identical with the human ASNase) that indeed shows a different conformation at the active site. However, the nucleophile crystallized in an inactive rotomeric state, and it was concluded that some conformational change must occur to populate a reactive state.[58]

Collectively, our analysis of the *cis*-autoproteolysis literature reveals that the existing data cannot rule out our hypothesis that self-cleavage proceeds through a *si*-face attack. To date, direct and mechanistically sound structural data supporting a *si*-face attack in clan PB exist for only PβS, and it will be crucial to confirm this mechanism for other enzymes. Application of room-temperature crystallography may aid in the observation of higher-energy states.[45] Even with this advance, the data presented here demonstrate that the standard approach of crystallizing inactive variants is unlikely to produce the evidence needed to discriminate between closely related mechanisms, and that additional techniques are needed in this pursuit.

■ CONCLUSIONS

Establishing the role of protein dynamics in reaction rate enhancement is a subject of intense interest and debate. We report here our observation and characterization of complex conformational coupling between the reaction center and neighboring loop motifs in the autoproteolytic site of ThnT. Our data provide evidence that unique conformational ensembles are associated with each reaction catalyzed by ThnT, and that autoproteolysis shifts the ensemble from one favoring self-cleavage to one tuned for substrate catalysis. The conformational coupling that allows this transition is strong enough that its disruption will impede the ability to identify a reactive state through X-ray crystallography. We argue that this may be a general phenomenon that is responsible for the unfortunate misinterpretation of inactive protein structures as being representative of a reactive state. We introduce the hypothesis that the N → O(S) acyl shift in *cis*-autoproteolysis always occurs through a *si*-face attack, thereby unifying the chemistry of autoproteolytic enzymes through a common mechanism. Additional data are needed to validate or refute this hypothesis. This work demonstrates the importance of protein conformational coupling in autoprocessing chemistry and makes clear the need for additional experimental tools for studying autoactivation.

■ ASSOCIATED CONTENT

Supporting Information

Figures showing the steric clash between L319 and G76 and the inhibition of proteolytic degradation by inclusion of a protease

dx.doi.org/10.1021/bi500385d | *Biochemistry* 2014, 53, 4273−4281

inhibitor cocktail and tables listing the primers used to generate the variants discussed here and the crystallographic data collection and refinement statistics. This material is available free of charge via the Internet at http://pubs.acs.org.

AUTHOR INFORMATION

Corresponding Author

*E-mail: ctownsend@jhu.edu. Telephone: (410) 516-7444.

Present Addresses

[‖]A.R.B.: Department of Chemical Engineering, California Institute of Technology, Pasadena, CA 91125.

[⊥]M.F.F.: Institute of Microbiology, Eidgenössische Technische Hochschule Zurich, Vladimir-Prelog-Weg 1-5/10, 8093 Zurich, Switzerland.

Funding

This work was supported by National Institutes of Health Grant R01 AI014937.

Notes

The authors declare no competing financial interest.

ACKNOWLEDGMENTS

We thank Dr. Courtney Hastings for long discussions of enzyme kinetics and Eyring analysis. We thank Professors Doug Barrick and Dominique Frueh for comments on early drafts of the manuscript and Belinda Wenke for careful editing. We gratefully acknowledge Dr. Vivian Stojanoff, Dr. Jean Jakonic, and Edwin Lazo at National Synchrotron Lightsource beamline X6A for assistance in data collection.

REFERENCES

(1) Fraser, J. S., Clarkson, M. W., Degnan, S. C., Erion, R., Kern, D., and Alber, T. (2009) Hidden alternative structures of proline isomerase essential for catalysis. *Nature 462*, 669−673.

(2) Henzler-Wildman, K. A., Thai, V., Lei, M., Ott, M., Wolf-Watz, M., Fenn, T., Pozharski, E., Wilson, M. A., Petsko, G. A., Karplus, M., Huebner, C. G., and Kern, D. (2007) Intrinsic motions along an enzymatic reaction trajectory. *Nature 450*, 838−844.

(3) Schrank, T. P., Bolen, D. W., and Hilser, V. J. (2009) Rational modulation of conformational fluctuations in adenylate kinase reveals a local unfolding mechanism for allostery and functional adaptation in proteins. *Proc. Natl. Acad. Sci. U.S.A. 106*, 16984−16989.

(4) Raber, M. L., Freeman, M. F., and Townsend, C. A. (2009) Dissection of the Stepwise Mechanism to β-Lactam Formation and Elucidation of a Rate-determining Conformational Change in β-Lactam Synthetase. *J. Biol. Chem. 284*, 207−217.

(5) Hammes-Schiffer, S., and Benkovic, S. J. (2006) Relating protein motion to catalysis. *Annu. Rev. Biochem. 75*, 519−541.

(6) Schwartz, S. D., and Schramm, V. L. (2009) Enzymatic transition states and dynamic motion in barrier crossing. *Nat. Chem. Biol. 5*, 552−559.

(7) Kipp, D. R., Silva, R. G., and Schramm, V. L. (2011) Mass-Dependent Bond Vibrational Dynamics Influence Catalysis by HIV-1 Protease. *J. Am. Chem. Soc. 133*, 19358−19361.

(8) Henzler-Wildman, K. A., Lei, M., Thai, V., Kerns, S. J., Karplus, M., and Kern, D. (2007) A hierarchy of timescales in protein dynamics is linked to enzyme catalysis. *Nature 450*, 913−916.

(9) Boehr, D. D., McElheny, D., Dyson, H. J., and Wright, P. E. (2006) The dynamic energy landscape of dihydrofolate reductase catalysis. *Science 313*, 1638−1642.

(10) Miller, M. T., Bachmann, B. O., Townsend, C. A., and Rosenzweig, A. C. (2002) The catalytic cycle of β-lactam synthetase observed by X-ray crystallographic snapshots. *Proc. Natl. Acad. Sci. U.S.A. 99*, 14752−14757.

(11) Collins, K. D., and Stark, G. R. (1971) Aspartate Transcarbamylase: Interaction with Transition State Analogue N-(Phosphonacetyl)-L-aspartate. *J. Biol. Chem. 246*, 6599−6605.

(12) Arac, D., Boucard, A. A., Bolliger, M. F., Nguyen, J., Soltis, S. M., Suedhof, T. C., and Brunger, A. T. (2012) A novel evolutionarily conserved domain of cell-adhesion GPCRs mediates autoproteolysis. *EMBO J. 31*, 1364−1378.

(13) Tinel, A., Janssens, S., Lippens, S., Cuenin, S., Logette, E., Jaccard, B., Quadroni, M., and Tschopp, J. (2007) Autoproteolysis of PIDD marks the bifurcation between pro-death caspase-2 and pro-survival NF-κB pathway. *EMBO J. 26*, 197−208.

(14) Rosenblum, J. S., and Blobel, G. (1999) Autoproteolysis in nucleoporin biogenesis. *Proc. Natl. Acad. Sci. U.S.A. 96*, 11370−11375.

(15) Sun, Y., and Guo, H. C. (2008) Structural constraints on autoprocessing of the human nucleoporin Nup98. *Protein Sci. 17*, 494−505.

(16) Blount, K. E., and Uhlenbeck, O. C. (2005) The structure-function dilemma of the hammer head ribozyme. In *Annual Review of Biophysics and Biomolecular Structure*, pp 415−440, Annual Reviews, Palo Alto, CA.

(17) Johansson, D. G. A., Macao, B., Sandberg, A., and Hard, T. (2008) SEA domain autoproteolysis accelerated by conformational strain: Mechanistic aspects. *J. Mol. Biol. 377*, 1130−1143.

(18) Sandberg, A., Johansson, D. G. A., Macao, B., and Hard, T. (2008) SEA domain autoproteolysis accelerated by conformational strain: Energetic aspects. *J. Mol. Biol. 377*, 1117−1129.

(19) Brannigan, J. A., Dodson, G., Duggleby, H. J., Moody, P. C. E., Smith, J. L., Tomchick, D. R., and Murzin, A. G. (1995) A Protein Catalytic Framework with an N-Terminal Nucleophile Is Capable of Self-Activation. *Nature 378*, 416−419.

(20) Cheng, H., and Grishin, N. V. (2005) DOM-fold: A structure with crossing loops found in DmpA, ornithine acetyltransferase, and molybdenum cofactor-binding domain. *Protein Sci. 14*, 1902−1910.

(21) Perler, F. B., Xu, M. Q., and Paulus, H. (1997) Protein splicing and autoproteolysis mechanisms. *Curr. Opin. Chem. Biol. 1*, 292−299.

(22) Zhiryakova, D., Ivanov, I., Ilieva, S., Guncheva, M., Galunsky, B., and Stambolieva, N. (2009) Do N-terminal nucleophile hydrolases indeed have a single amino acid catalytic center? *FEBS J. 276*, 2589−2598.

(23) Duggleby, H. J., Tolley, S. P., Hill, C. P., Dodson, E. J., Dodson, G., and Moody, P. C. E. (1995) Penicillin Acylase Has a Single-Amino-Acid Catalytic Center. *Nature 373*, 264−268.

(24) Smith, J. L., Zaluzec, E. J., Wery, J. P., Niu, L. W., Switzer, R. L., Zalkin, H., and Satow, Y. (1994) Structure of the Allosteric Regulatory Enzyme of Purine Biosynthesis. *Science 264*, 1427−1433.

(25) Lowe, J., Stock, D., Jap, R., Zwickl, P., Baumeister, W., and Huber, R. (1995) Crystal Structure of the 20S Proteasome from the Archaeon *T. acidophilum* at 3.4-Å Resolution. *Science 268*, 533−539.

(26) Rawlings, N. D., Barrett, A. J., and Bateman, A. (2012) MEROPS: The database of proteolytic enzymes, their substrates and inhibitors. *Nucleic Acids Res. 40*, D343−D350.

(27) Ditzel, L., Huber, R., Mann, K., Heinemeyer, W., Wolf, D. H., and Groll, M. (1998) Conformational constraints for protein self-cleavage in the proteasome. *J. Mol. Biol. 279*, 1187−1191.

(28) Buller, A. R., and Townsend, C. A. (2013) Intrinsic evolutionary constraints on protease structure, enzyme acylation, and the identity of the catalytic triad. *Proc. Natl. Acad. Sci. U.S.A. 110*, E653−E661.

(29) Freeman, M. F., Moshos, K. A., Bodner, M. J., Li, R. F., and Townsend, C. A. (2008) Four enzymes define the incorporation of coenzyme A in thienamycin biosynthesis. *Proc. Natl. Acad. Sci. U.S.A. 105*, 11128−11133.

(30) Buller, A. R., Freeman, M. F., Wright, N. T., Schildbach, J. F., and Townsend, C. A. (2012) Insights into cis-autoproteolysis reveal a reactive state formed through conformational rearrangement. *Proc. Natl. Acad. Sci. U.S.A. 109*, 2308−2313.

(31) Okada, T., Suzuki, H., Wada, K., Kumagai, H., and Fukuyama, K. (2007) Crystal structure of the γ-glutamyltranspeptidase precursor protein from *Escherichia coli*: Structural changes autocatalytic

processing and implications for the maturation mechanism. *J. Biol. Chem. 282*, 2433−2439.
(32) Michalska, K., Hernandez-Santoyo, A., and Jaskolski, M. (2008) The mechanism of autocatalytic activation of plant-type L-asparaginases. *J. Biol. Chem. 283*, 13388−13397.
(33) Khan, J. A., Dunn, B. M., and Tong, L. (2005) Crystal structure of human Taspase1, a crucial protease regulating the function of MLL. *Structure 13*, 1443−1452.
(34) Buller, A. R., Labonte, J. W., Freeman, M. F., Wright, N. T., Schildbach, J. F., and Townsend, C. A. (2012) Autoproteolytic Activation of ThnT Results in Structural Reorganization Necessary for Substrate Binding and Catalysis. *J. Mol. Biol. 422*, 508−518.
(35) Otwinowski, Z., and Minor, W. (1997) Processing of X-ray diffraction data collected in oscillation mode. *Methods Enzymol. 276*, 307−326.
(36) McCoy, A. J., Grosse-Kunstleve, R. W., Adams, P. D., Winn, M. D., Storoni, L. C., and Read, R. J. (2007) Phaser crystallographic software. *J. Appl. Crystallogr. 40*, 658−674.
(37) Emsley, P., and Cowtan, K. (2004) Coot: Model-building tools for molecular graphics. *Acta Crystallogr. D60*, 2126−2132.
(38) Winn, M. D., Murshudov, G. N., and Papiz, M. Z. (2003) Macromolecular TLS refinement in REFMAC at moderate resolutions. *Methods Enzymol. 374*, 300−321.
(39) Painter, J., and Merritt, E. A. (2006) TLSMD web server for the generation of multi-group TLS models. *J. Appl. Crystallogr. 39*, 109−111.
(40) Chen, V. B., Arendall, W. B., III, Headd, J. J., Keedy, D. A., Immormino, R. M., Kapral, G. J., Murray, L. W., Richardson, J. S., and Richardson, D. C. (2010) MolProbity: All-atom structure validation for macromolecular crystallography. *Acta Crystallogr. D66*, 12−21.
(41) Ramachandran, G. N., and Mitra, A. K. (1976) Explanation for Rare Occurrence of cis Peptide Units in Proteins and Polypeptides. *J. Mol. Biol. 107*, 85−92.
(42) Henzler-Wildman, K., and Kern, D. (2007) Dynamic personalities of proteins. *Nature 450*, 964−972.
(43) Boehr, D. D., Dyson, H. J., and Wright, P. E. (2006) An NMR perspective on enzyme dynamics. *Chem. Rev. 106*, 3055−3079.
(44) Tzeng, S.-R., and Kalodimos, C. G. (2012) Protein activity regulation by conformational entropy. *Nature 488*, 236−240.
(45) Fraser, J. S., van den Bedem, H., Samelson, A. J., Lang, P. T., Holton, J. M., Echols, N., and Alber, T. (2011) Accessing protein conformational ensembles using room-temperature X-ray crystallography. *Proc. Natl. Acad. Sci. U.S.A. 108*, 16247−16252.
(46) Fraser, J. S., and Jackson, C. J. (2011) Mining electron density for functionally relevant protein polysterism in crystal structures. *Cell. Mol. Life Sci. 68*, 1829−1841.
(47) Wand, A. J. (2013) The dark energy of proteins comes to light: Conformational entropy and its role in protein function revealed by NMR relaxation. *Curr. Opin. Struct. Biol. 23*, 75−81.
(48) Lewis, C. A., and Wolfenden, R. (2011) Amide Bonds to the Nitrogen Atoms of Cysteine and Serine as "Weak Points" in the Backbones of Proteins. *Biochemistry 50*, 7259−7264.
(49) Guan, C. D., Cui, T., Rao, V., Liao, W., Benner, J., Lin, C. L., and Comb, D. (1996) Activation of glycosylasparaginase: Formation of active N-terminal threonine by intramolecular autoproteolysis. *J. Biol. Chem. 271*, 1732−1737.
(50) Scott, W. G., Murray, J. B., Arnold, J. R. P., Stoddard, B. L., and Klug, A. (1996) Capturing the structure of a catalytic RNA intermediate: The hammerhead ribozyme. *Science 274*, 2065−2069.
(51) Scott, W. G., Finch, J. T., and Klug, A. (1995) The Crystal Structure of an All-RNA Hammerhead Ribozyme: A Proposed Mechanism for RNA Catalytic Cleavage. *Cell 81*, 991−1002.
(52) Martick, M., and Scott, W. G. (2006) Tertiary contacts distant from the active site prime a ribozyme for catalysis. *Cell 126*, 309−320.
(53) Nelson, J. A., and Uhlenbeck, O. C. (2006) When to believe what you see. *Mol. Cell 23*, 447−450.
(54) Merz, T., Heck, T., Geueke, B., Mittl, P. R. E., Briand, C., Seebach, D., Kohler, H.-P. E., and Grutter, M. G. (2012) Autoproteolytic and Catalytic Mechanisms for the β-Aminopeptidase BapA-A Member of the Ntn Hydrolase Family. *Structure 20*, 1850−1860.
(55) Paulus, H. (2000) Protein splicing and related forms of protein autoprocessing. *Annu. Rev. Biochem. 69*, 447−496.
(56) Wang, Y. M., and Guo, H. C. (2010) Crystallographic Snapshot of Glycosylasparaginase Precursor Poised for Autoprocessing. *J. Mol. Biol. 403*, 120−130.
(57) Su, Y., Karamitros, C. S., Nomme, J., McSorley, T., Konrad, M., and Lavie, A. (2013) Free glycine accelerates the autoproteolytic activation of human asparaginase. *Chem. Biol. 20*, 533−540.
(58) Schalk, A. M., and Lavie, A. (2014) Structural and Kinetic Characterization of Guinea Pig L-Asparaginase Type III. *Biochemistry 53*, 2318−2328.